STREAMLINE.
OPTIMIZE.
TRUST.


ADAPTIVO


LINACVIEW


DOSEVIEW


PIPSPRO


QA PILOT

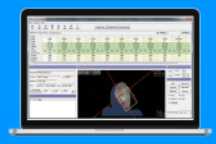
IMSURE

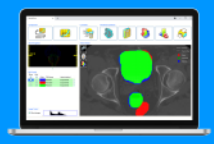
STRUCTSURE AI QA

COMPLETE INTEGRATED QA

STANDARD IMAGING®

CLICK HERE TO LEARN MORE

Received: 27 October 2020 | Revised: 21 April 2021 | Accepted: 9 June 2021

DOI: 10.1002/mp.15080

MEDICAL PHYSICS

TECHNICAL NOTE

Technical note: Validation of 3D ultrasound for image registration during oncological liver surgery

Jasper N. Smit[1] | **Koert F. D. Kuhlmann**[1] | **Bart R. Thomson**[1] | **Niels F. M. Kok**[1] | **Matteo Fusaglia**[1] | **Theo J. M. Ruers**[1,2]

[1]Department of Surgical Oncology, The Netherlands Cancer Institute – Antoni van Leeuwenhoek, Amsterdam, The Netherlands

[2]Faculty of Science and Technology (TNW), Nanobiophysics group (NBP), University of Twente, NB Enschede, The Netherlands

Correspondence
Jasper N. Smit, The Netherlands Cancer Institute – Antoni van Leeuwenhoek, Department of Surgical Oncology, A.2.309, Plesmanlaan 121, 1066CX Amsterdam, The Netherlands.
Email: j.smit@nki.nl

Funding information
The authors received no specific funding for this work.

Abstract

Purpose: Registration of pre- and intraoperative images is a crucial step of surgical liver navigation, where rigid registration of vessel centerlines is currently commonly used. When using 3D ultrasound (US), accuracy during navigation might be influenced by the size of the intraoperative US volume, yet the relationship between registration accuracy and US volume size is understudied. In this study, we specify an optimal 3D US volume size for registration using varying volumes of liver vasculature. While previous studies measured accuracy at registered fiducials, in this work, accuracy is determined at the target lesion which is clinically the most relevant structure.

Methods: Three-dimensional US volumes were acquired in 14 patients after laparotomy and liver mobilization. Manual segmentation of vasculature and centerline extraction was performed. Intraoperative and preoperative vasculature centerlines were registered with coherent point drift, using different sub-volumes (sphere with radius r = 30, 40, …, 120 mm). Accuracy was measured by fiducial registration error (FRE) between vessel centerlines and target registration error (TRE) at the center of the target lesion.

Results: The lowest FRE for vessel registration was reached with r = 50 mm (6.5 ± 2.5 mm), the highest with r = 120 mm (7.1 ± 2.1 mm). Clinical accuracy at the target lesion, resulted most accurate (TRE = 8.8 ± 5.0 mm) in sub-volumes with a radius of 50 mm. Smaller US sub-volumes resulted in lower average TREs when compared to larger US sub-volumes (Pearson's correlation coefficient R = 0.91, p < 0.001).

Conclusion: Our results indicate that there is a linear correlation between US volume size and registration accuracy at the tumor. Volumes with radii of 50 mm around the target lesion yield higher accuracy (p < 0.05) (Trial number IRBd18032, 11 September 2018).

KEYWORDS
3D ultrasound, image-guided surgery, liver surgery, registration

Abbreviations: 2D, two-dimensional; 3D, three-dimensional; CPD, coherent point drift; CRLM, colorectal liver metastasis; CT, computed tomography; FRE, fiducial registration error; ICP, iterative closest point; MRI, magnetic resonance imaging; RMSE, root-mean-squared error; STL, standard triangle language; TRE, target registration error; US, ultrasound.

1 | INTRODUCTION

Annually approximately 1 million patients develop malignant liver lesions from primary cancer worldwide.[1] Additionally, liver metastases occur in up to 50% of the patients with primary colorectal cancer.[2] When feasible, the preferred treatment of these lesions is surgical resection.[3] During surgery, radical resection (i.e., no tumor tissue is left behind) is the key to ensure local disease-free survival. To achieve radical tumor resection, tumor boundaries are determined through palpation and ultrasound (US) imaging. The location of the tumor within the liver, tumor origin, and neo-adjuvant treatment may limit the effectiveness of these methods. Tumors which are deep seated, as well as comparatively small lesions, are non-palpable and under these circumstances only US allows for accurate tumor localization.[4] However, in case of isoechoic lesions or vanishing tumor lesions, also the use of US is limited. Isoechoic lesions (i.e., tumors which appear as parenchyma on US) occur in 10% of colorectal liver metastases,[5] while vanishing lesions (i.e., tumors which shrink due to neo-adjuvant chemotherapy) occur in 9% of the patients who receive preoperative chemotherapy.[6] In these cases where conventional ways of intraoperative tumor localization obviously fail, surgical navigation technology may be of use.

Surgical navigation aims at localizing these tumor lesions by presenting preoperative imaging within the intraoperative field. To this end, preoperative images, intraoperative organ position, and surgical instruments are displayed in the same coordinate system. This enables the surgeon to take advantage of the properties of preoperative imaging, such as the sensitivity of magnetic resonance imaging (MRI) for subcentimeter lesions, and apply this knowledge intraoperatively. Isoechoic and vanishing tumors which are visible in the preoperative scene can now be localized during surgery. In addition, by showing the position of deep-seated non-palpable tumors with respect to the surrounding hepatic vasculature, these tumors can be clearly visualized and resected or ablated with sufficient tumor-free margins.

Important steps in the workflow of surgical navigation are to generate an intraoperative 3D imaging volume of the liver and the tumor lesions and to determine the position of this 3D volume within a navigation coordinate system. The preferred method for intraoperative liver imaging is via US, since it is real time, relatively cheap, radiation-free, and can be well-integrated within the surgical workflow. By coupling of an US probe with a tracking sensor, it also enables to represent the position of the images in a navigation coordinate system. For the acquisition of an accurate 3D volume of the liver by US, two main approaches have been described.

In one approach the US probe is coupled with a tracking sensor that allows for US tomography by means of stacking a series of tracked two-dimensional (2D) images (i.e., freehand US).[7–9] Hepatic vasculature can be segmented from the intraoperative US tomography, resulting in an intraoperative 3D model of the underlying hepatic vasculature that can be registered with its preoperative counterpart. This methodology, tested in different clinical studies, sometimes causes inadequate volume reconstruction due to suboptimal interpolation of the stacked 2D images.[10,11] Additionally, variations in maneuvering the US transducer during the sweep induce additional liver deformations which can affect the registration accuracy.

Alternatively, US transducers equipped with arrays of 2D piezoelectric elements can be used to generate a 3D pyramidal frustum-shaped US tomography (i.e., 3D transducers).[12] A disadvantage of 3D transducers is their large size, due to the increased number of piezoelectric elements. As a result, 3D transducers are mainly used for percutaneous examinations rather than direct measurements on the liver,[13–15] hence their use in the context of liver navigation is scarce. Nevertheless, 3D transducers are appealing devices for acquiring the intraoperative liver position, since they can be hold statically on the liver surface, show fast acquisition times, and generally allow a superior reconstruction quality when compared to freehand tracked 2D US.

Consecutive to image acquisition, the 3D volume needs to be registered to the preoperative images by geometrical mapping between the preoperative imaging and the intraoperative organ position. Obtaining an accurate registration is a key aspect for successful implementation of surgical navigation within the clinical routine. Registration can be performed on liver contour and anatomical structures like vessel anatomy. Respiratory motion, organ deformation, and laparotomy itself, however, will change the intraoperative position and shape of the liver with respect to the preoperative situation, which clearly hinders the registration accuracy.

In this study, we aim to evaluate the registration accuracy of acquired 3D US volumes during open liver surgery and explore possible constraints with respect to the volume of registration. We expect that 3D US provides locally accurate registration of 10 mm or less at the tumor since deformation is limited during the static and fast acquisition of 3D US.

We hypothesize that the vessel-based registration is more accurate when using smaller sub-volumes of the vasculature around the lesion. To this end, we investigate the registration accuracy using varying sub-volumes of liver vasculature in order to specify an optimal size of 3D US volume for registration. We investigate if there is a relation between volume size and target registration error (TRE) at the tumor. As opposed to earlier studies, which mostly determined accuracy

on vessel bifurcations,[7,9,16] we validated the accuracy on target lesions as well, as this is clinically the most relevant measure.

2 | MATERIALS AND METHODS

2.1 | Patient population

This was a prospective feasibility study of patients with malignant liver lesions from any origin conducted at the Netherlands Cancer Institute––Antoni van Leeuwenhoek hospital. Patients of 18 years and older scheduled for tumor resection by open liver surgery were eligible candidates in this study. Patients were required to have at least one visible lesion during preoperative imaging, that was judged to be also visible on intraoperative US. Preoperative imaging consisted of computed tomography (CT) or MRI with clear contrast between hepatic structures.

The trial protocol was approved by the institutional review board with a waiver of informed consent in September 2018 (trial number IRBd18032). Sixteen patients were included in a period of 7 months.

2.2 | Intraoperative measurement

A Philips EPIQ7 (Philips Ultrasound) US scanner with a X6-1 xMATRIX phased array transducer (center frequency 3.5 MHz) was used to acquire B-mode 3D volumes of the liver. The transducer, with a flat contact surface of 4 × 3 cm, was put inside a sterile cover and was placed on the liver surface during laparotomy, once the liver was fully exposed after limited mobilization. The surgeon was asked to apply minimal pressure on the transducer, limiting further local deformation. Scanning depth was set between 7 and 16 cm depending on the tumor location to capture sufficient amounts of vascularity, together with the targeted liver lesion. The field of view was kept constant and set to a maximum aperture of 90° × 90° × 100°. Acquired image resolution varied between 0.24 × 0.18 × 0.43 mm (480 × 409 × 256 voxels) and 0.48 × 0.42 × 0.93 mm (512 × 397 × 256 voxels) voxel grid, for 7 and 16 cm depth, respectively. Harmonic imaging was enabled, and the gain was increased by approximately 25% in cases of low superficial contrast. XRES adaptive image processing, available on the EPIQ7 machine, was enabled during acquisition which reduced speckle, haze, and clutter artifacts.[17]

Geometric accuracy of the US transducer was verified using the tissue-equivalent ATS 570 phantom (Computerized Imaging Reference Systems, Inc.) according to Dutch guidelines on image quality assessment for radiological equipment.[18,19] This phantom contains distance markers which were used for distance measurements and resulted in a mean relative error of 1.9 ± 0.4% in the coronal plane of acquisition (range: 1.4%–2.4%, measured in nine volumes), and 6.1 ± 0.8% in the axial plane (range: 4.8%–7.2%, n = 9). The distance calibration error was considered sufficiently accurate for the purpose of this study as it was smaller than the voxel size.

2.3 | Image processing

For each patient, a preoperative CT or MRI scan was used for vessel and tumor segmentation for visual guidance during surgery, which is a standard clinical care in this institute.[20] MRI scans were semi-automatically segmented using a custom-built version of Slicer.[21,22] Segmentation of CT images was performed with IntelliSpace Portal (Philips Healthcare), using the liver segmentation module.[23] In this software, vessels are delineated automatically and were manually corrected where needed. Target lesions were delineated manually using a region-growing brush.

The intraoperatively acquired 3D US volumes were manually delineated. Using Slicer's Segment Editor Widget, lesions were manually delineated in all axial slices. Correct delineation was visually confirmed in corresponding coronal and sagittal slices at the tumor location.

Subsequently, hepatic and portal veins were segmented using a local thresholding brush in Slicer's Segment Editor Widget. These segmentations often contained small islands that did not belong to a vascular model. These islands, between 1 and 3 mm in diameter, were removed using a median filter with a kernel of 3 × 3 × 3 voxels. A Python implementation of the skeletonization algorithm by Lee et al.[24] iterates over the segmented vascular model with a 3 × 3 × 3 voxel kernel, removing voxels at each iteration until the output stops changing. This resulted in extraction of the centerlines from both the preoperative and the intraoperative segmentations (Figure 2a). Both centerlines were represented as a set of discrete points.

2.4 | Registration and accuracy

Prior to the automatic registration, an initial alignment of the two vasculature trees was applied. This initial manual alignment was performed manually by overlaying the preoperative vasculature onto its intraoperative counterpart by translation and rotation using Slicer's Transformations Widget, and was performed by technical medical staff which performs preoperative planning on a regular basis. Centerlines of the vessel trees from preoperative imaging were downsampled to 50% to improve the accuracy and computational efficiency of registration. Subsequently, coherent point drift (CPD)

was used to register the two centerlines.[25] An outlier ratio of 30% was determined because of the non-uniform distribution of the point cloud. Iteration of the CPD algorithm ends when the maximum of 200 iterations was reached or if a termination tolerance between consecutive CPD iterations of 1×10^{-4} was reached.

Different sizes of point clouds were used to evaluate the influence of the amount of vasculature that was present around the lesion on the registration accuracy. Starting at the center of the lesion in the US volume, a sphere with a varying radius (r = 30, 40, …, 120 mm) was determined (Figure 1). Centerline points enclosed in this sphere were used for registration.

To measure accuracy of the vessel registration, the fiducial registration error (FRE) was calculated as root-mean-squared error between centerlines. After registration, the resulting transformation was applied on the center of the preoperative target lesion. Clinical accuracy of the registration, defined as the TRE, was calculated as the Euclidean distance between the center of the target lesion in the registered preoperative scan, and the center of the target lesion in the intraoperative US volume. In 12 patients the target lesion was a liver metastasis. In one case a cyst was used as target lesion and in one case a hemangioma, because the liver metastases were isoechoic.

The sign test (α = 0.05) was used to test the hypothesis of achieving a median TRE of 10 mm. The Pearson's linear correlation coefficient was calculated to determine correlation between the registration errors (FRE and TRE) and registration volume size. Significance was defined at the $p < 0.05$ level. Additionally, the Pearson's correlation coefficient was calculated between the TRE and (1) the distance of the target lesion to the closest vessel; (2) diameter of the lesion; (3) the distance of the lesion to the surface of the liver; and (4) the distance of the lesion to the US transducer's surface. Additionally, difference per patient between volumes was tested used Wilcoxon signed rank t-test for paired data, with significance level α = 0.05. No adjustment for multiplicity was performed due to the small sample size.

Changes in (log)TRE for different volume radii accounting for the correlation between the repeated measurements of each patient were assessed using a linear mixed-effects model. A nonlinear effect of the radius was allowed using restricted cubic splines. Results were adjusted for tumor depth with respect to the US transducer, and interactions were considered. Likelihood ratio tests were considered to select the best fixed- and random-effect structure.

3 | RESULTS

In 14 patients, the target lesion was visible in the acquired US scans. In two, it was not possible to delineate the lesion due to isoechogeneity. Median diameter of the lesion was 17.1 mm (range: 5.1–55.0 mm). Lesions were located in segments I and IV–VIII, with a median depth of 25.6 mm below the liver surface (range: 7.6–41.7 mm). The US volumes were acquired with a median scanning depth of 11 cm (range: 7–16 cm).

A 3D visualization of an US scan is shown in Figure 2a where vasculature and the target lesion are delineated in the US scan. The location of the US

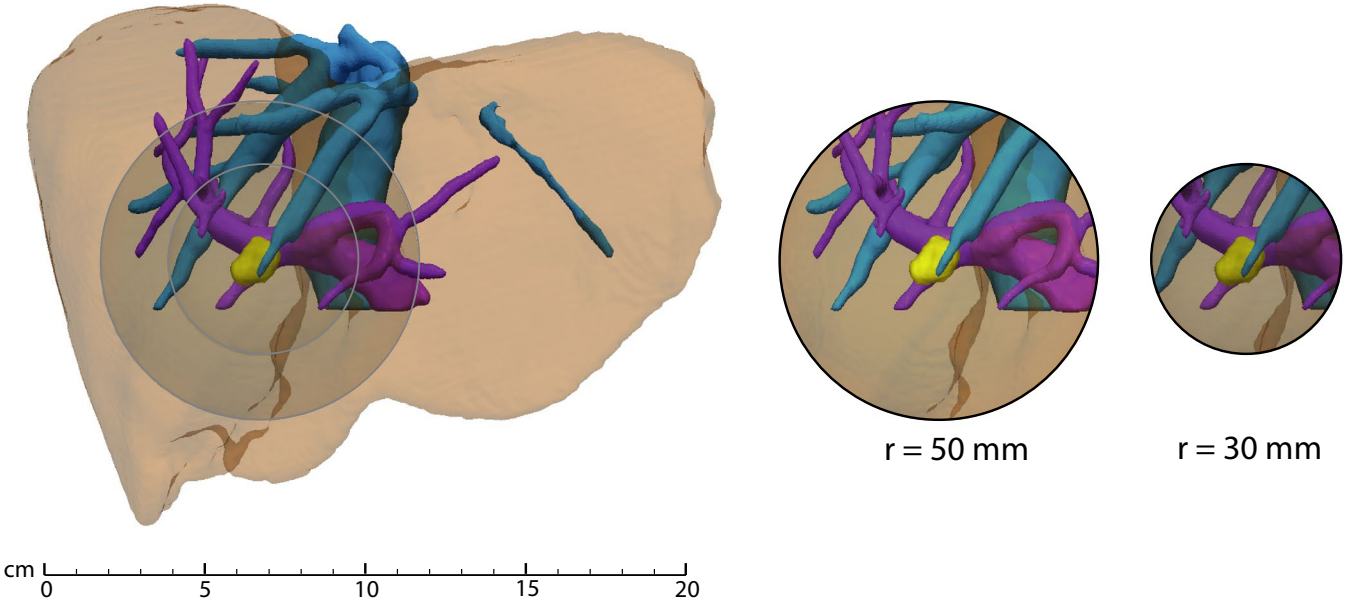

FIGURE 1 Three-dimensional (3D) model of the liver based on a preoperative scan. Spheres with varied radii starting at the center of the target lesion (yellow) were used for registration of the 3D ultrasound volume. Selected spheres include different amounts of portal (purple) and hepatic (blue) vasculature

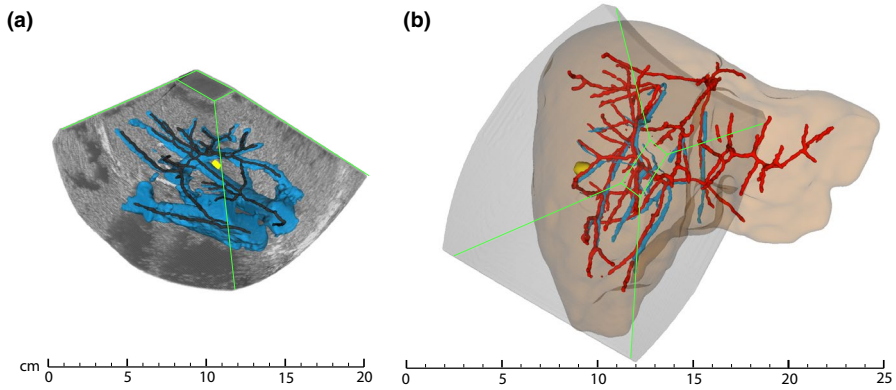

FIGURE 2 (a) Visualization of the pyramidal frustum-shaped three-dimensional (3D) ultrasound volume, containing vasculature (blue) with centerlines (black) and a tumor lesion (yellow). (b) 3D model based on the preoperative scan with centerlines from vasculature (red) and the lesion (yellow). The mask of the ultrasound volume (gray) with the centerlines from segmented vasculature (blue) depict the location of where the ultrasound transducer was placed for acquisition during surgery before registration

FIGURE 3 Boxplot of the registration accuracy of lesions (red, TRE) and vasculature (blue, FRE), when the radius of the point cloud is varied between 30 and 120 mm. The median (stripe) and average (diamonds) are plotted, as well as outliers (black circles)

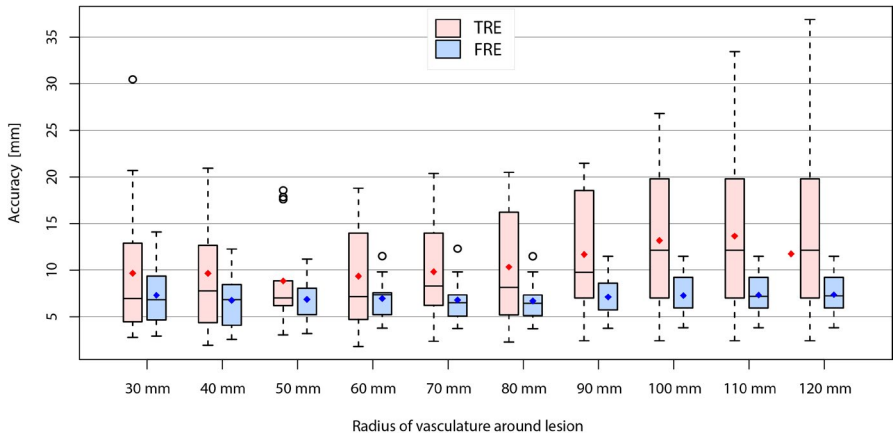

volume with respect to the liver anatomy after initial alignment is illustrated in Figure 2b.

Figure 3 shows the registration accuracy between preoperative and intraoperative centerlines of the vasculature (FRE) and the clinical accuracy at the target lesion (TRE), both in relation to the radius of the registration volume. The average FRE for the centerlines of the vasculature was 6.7 ± 2.4 mm, and was quite constant using different registration volumes. The lowest average FRE for vessel registration was reached with r = 50 mm (6.5 ± 2.5 mm) and the highest with r = 120 mm (7.1 ± 2.1 mm).

For the clinical accuracy, smaller registration volumes resulted in lower average TREs when compared to larger registration volumes (correlation coefficient R = 0.91, p = 0.0003, 95% CI: 0.65–0.98).

Average TRE values remained below 10 mm for registration volumes with a radius below 80 mm, at or above a radius of 80 mm TRE values higher than 10 mm were noticed. Average TRE was found to be the lowest in the range 50–60 mm (8.8 ± 5.0 and 9.4 ± 5.7 mm). The sign test (α = 0.05) showed that only volumes with a radius of 50 mm resulted in a confirmation of the hypothesis that a median TRE lower than 10 mm could be achieved (p = 0.029).

An overlap in distributions of TRE values is visible for different radii in Figure 3. The Wilcoxon t-test for paired data showed a significant difference between the TREs found when comparing volumes with radii of 50 and 120 mm (p = 0.034). Additionally, a significant difference was found between the TREs in 80 and 90 mm volumes (p = 0.016). Comparing TRE values in volumes of 50 and 60 mm did not result in a significant difference (p = 0.42).

One case using different amounts of vasculature after CPD registration is shown in Figure 4. Larger (r = 100 mm) and smaller (r = 40 mm) amounts of vasculature resulted in TREs of 24.1 and 4.4 mm, respectively.

Since US volumes with radii of 50 mm resulted in the lowest TRE, a possible relation between the location of the target lesion and the TRE was investigated by means of the Pearson's correlation coefficient. No significant correlation was found between the TRE and the

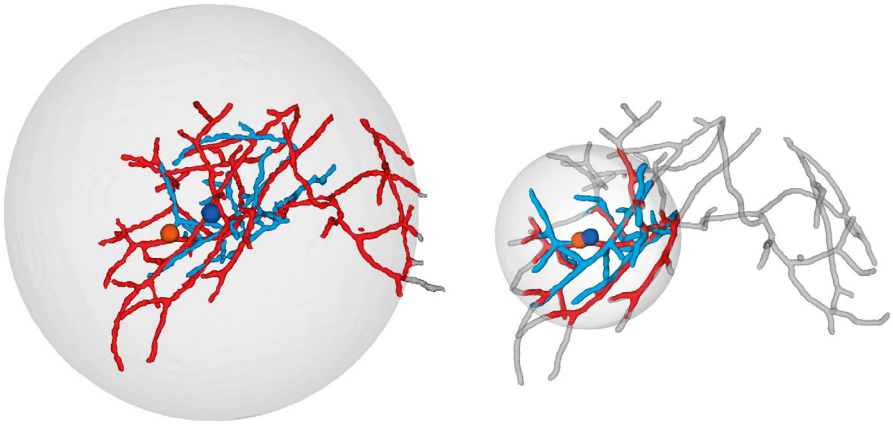

FIGURE 4 Registered preoperative (red) and intraoperative (blue) vasculature trees with their lesions in corresponding colors. On the left, registration of all centerline points within a radius of 100 mm resulted in a TRE of 24.1 mm. On the right, registration using a sphere with a radius of 40 mm (gray circle) resulted in a TRE of 4.4 mm

distance of the lesion to the closest vessel (correlation coefficient R = 0.14, p = 0.64, 95% CI: −0.43 to 0.62). Additionally, no significant correlation was found between the TRE and the diameter of the lesion (R = 0.15, p = 0.61, 95% CI: −0.41 to 0.63) or between the TRE and the distance to the surface of the liver (R = 0.12, p = 0.68, 95% CI: −0.44 to 0.61). No correlation was found between the TRE and the distance of the lesion to the US transducer for the volumes with r = 50 mm (R = 0.19, p = 0.51, 95% CI: −0.38 to 0.65). Also, for larger volumes with r = 120 mm this was not the case. (R = 0.28, p = 0.35, 95% CI: −0.30 to 0.70). Moreover, no significant correlations were found between the TRE and previously mentioned factors when US volumes with other radii were used. No correlation was found between the TRE and FRE (R = 0.44, p = 0.201, 95% CI: −0.26 to 0.84).

An indication of a linear trend of radius was found using a linear mixed-effects model (on average 5% increase in TRE for each 10 mm increase in radius, p = 0.075). TRE was found to be significantly lower for radii of 70 mm or lower with respect to 80 mm or higher (beta = −0.19, 95% CI −0.32 to −0.06, p = 0.0058). These results remained after adjusting for depth of the lesion with respect to the US transducer.

4 | DISCUSSION

Registration of pre- and intraoperative images is a crucial step of surgical navigation. In navigated liver surgery, rigid registration of vessel centerlines to align pre- and intraoperative images is currently commonly used since the organ is characterized by a complex vascular tree. Accuracy during navigation will be influenced by the size of the intraoperative US volume that will be taken into account during registration, yet it is understudied.

Our results show that using smaller 3D US volumes, with an optimal volume size with a radius of 50 mm, a more consistent accuracy is achieved with a lower standard deviation due to limited effects of liver deformation. While rigid registration in larger 3D US volumes results in a generally better overlap, it does not compensate for deformation and decreases the accuracy at the edges of the volume.

Three-dimensional US acquisition has demonstrated to acquire large amounts of vasculature in a volume, which can be used for vessel registration. Movement of the liver during acquisition, which affects the registration accuracy, is circumvented using static 3D US at the moment of controlled liver mobilization. Centerline extraction and registration based on the centerlines of these vessel trees showed a large overlap between centerlines extracted from the preoperative and intraoperative imaging, which is confirmed by consistent low FREs and standard deviations. An FRE of 6.7 mm is comparable to literature where FREs of 4.4–6.5 mm were demonstrated,[16,26] therefore, validating the methodology. However, a clear discrepancy in registration accuracy is shown between vasculature and target lesions, since vasculature registration with low FRE is not always followed by accurate target registration.

We show that target lesion registration tends to be more accurate in smaller registration volumes as shown in Figure 3. A clinically acceptable TRE at the location of the target lesion of less than 10 mm can be achieved when registration volumes with radii of 30–70 mm are used. This is most clearly noticeable using US volumes with r = 50 mm, as volumes with these radii resulted in acceptable TREs below 10 mm (p = 0.0287).

When US volumes with r = 50 mm was used for registration, three outliers (resulting in a mean TRE of 18 mm) were noticed, in which the target lesion was located in segment IV, centrally in segment VIII, and dorsally in segment VII. Since no correlation was found between the TRE and factors such as the distance to the closest vessel, distance to the surface, or the

diameter of the target lesion, the three outliers can be explained by liver deformation that affects the rigid registration accuracy locally near the target lesion. Such liver deformations may result from compression of liver tissue by the US transducer, for example, in case liver lesions are difficult to reach by the transducer, or may result from dissection of the liver which considerably changes the shape of the organ.

Coherent point drift as implemented in this workflow seems to cope with the dissimilarity of the point cloud sizes in most cases. When smaller volumes were used, CPD is sufficient. Nevertheless, CPD could not always handle the large dissimilarities and misalignment of the centerlines in larger volumes was prevalent where higher TRE values were found in volumes with a radius of 80 mm or higher ($p = 0.0058$). Based on early experiments, it was required to perform an initial rough alignment of the vessels. This helps to reduce the possibility of misalignment, due to the sensitivity of the CPD algorithm of converging to local minima.[25]

A strength of this study is that clinical accuracy is measured at relevant structures, that is, the targeted lesions, while previous research emphasized mainly on accuracy assessment of the registered vasculature.[7,9,16] In addition to accuracy assessment on the vasculature using the bifurcations, the accuracy is measured with regard to the position of the target lesion (Figure 3) which ultimately is the most clinically relevant parameter. Another strength is that the risks of inaccurate registration due to incorrect image reconstruction of EM-tracked 2D imaging is circumvented using static 3D US, resulting in quick 3D US acquisition which limits the effects of breathing and motion in the scan. This is different when using freehand US reconstruction, where the transducer is required to move during acquisition. In the setting of open liver surgery, the highly deformable liver is moving during the acquisition due to breathing and manipulation by the surgeon. When no organ tracking is provided, the movement inevitably leads to false image reconstruction of vasculature.

Registration accuracy is just one component in the overall accuracy of a navigation system. As the focus of this study was the acquisition of 3D US for registration, no tracking was performed and further navigation was not investigated. As other factors such as image segmentation quality, electromagnetic disturbance, and tool calibration will influence the overall accuracy, liver deformation will cause largest challenges in an accurate navigated procedure. Despite the postoperative setting of this study, registration with this methodology takes approximately a minute. This implies that when too much error is present, a re-registration can be performed quickly with 3D US.

The main limitation of this study is that segmentation has been performed manually, to minimize the possible effects of incorrect automatic segmentation or erroneous centerline extraction. This would not be possible during intraoperative use. Therefore, the use of automatic vessel and centerline extraction is recommended.[27] Another limitation is the cost of this transducer type, and might be a factor in clinical uptake of this technique. Additionally, the initial alignment was performed manually, which would not be feasible during surgery. Automatic initial registration showing sufficient rough alignment of structures has been attempted,[8] and is aimed for as a next step in our workflow.

5 | CONCLUSION

This study is the first clinical validation of 3D US for registration use during open liver surgery where a sufficient amount of patients was used. After laparotomy and mobilization of the liver, static 3D US has a good potential for intraoperative use for lesions surrounded by vasculature. Results show that for US volumes with a radius of 50 mm around a lesion that contain vasculature, we conclude that an optimal registration with a consistent accuracy is achieved. In these cases, accurate registration of less than 10 mm TRE can be achieved ($p < 0.05$).

ACKNOWLEDGMENTS

The authors thank Philips Healthcare, including Pedro Sanches, for providing us with the opportunity to use the EPIQ7 ultrasound system for research purposes.

CONFLICT OF INTEREST

The Netherlands Cancer Institute–Antoni van Leeuwenhoek has a research agreement with Philips Healthcare. Philips was not involved in the design and performance of this study.

AUTHOR CONTRIBUTION

Conceptualization: Smit, Fusaglia, Kuhlmann, and Ruers; Methodology: Smit, Kuhlmann, Fusaglia, Thomson, and Ruers; Formal analysis and investigation: Smit, Kuhlmann, Kok, and Ruers, Thomson; Writing––original draft preparation: Smit, Fusaglia, and Ruers; Writing––review and editing: Smit, Kuhlmann, Thomson, Kok, Fusaglia, and Ruers.

ETHICAL APPROVAL AND INFORMED CONSENT

The trial protocol was approved by the institutional review board of the Netherlands Cancer Institute–Antoni van Leeuwenhoek with a waiver of informed consent in September 2018 (trial number IRBd18032).

DATA AVAILABILITY STATEMENT

The data that support the findings of this study are available upon request from the corresponding author. The data are not publicly available due to privacy or ethical restrictions.

REFERENCES

1. Liu Z, Jiang Y, Yuan H, et al. The trends in incidence of primary liver cancer caused by specific etiologies: results from the Global Burden of Disease Study 2016 and implications for liver cancer prevention. *J Hepatol*. 2019;70(4):674–683. https://doi.org/10.1016/j.jhep.2018.12.001
2. van de Velde CJH. Treatment of liver metastases of colorectal cancer. *Ann Oncol*. 2005;16:ii144–ii149. https://doi.org/10.1093/annonc/mdi702
3. Taylor A, Primose JN, Langeberg W, et al. Survival after liver resection in metastatic colorectal cancer: review and meta-analysis of prognostic factors. *Clin Epidemiol*. 2012;4(1):283-301. https://doi.org/10.2147/CLEP.S34285
4. Hata S, Imamura H, Aoki T, et al. Value of visual inspection, bimanual palpation, and intraoperative ultrasonography during hepatic resection for liver metastases of colorectal carcinoma. *World J Surg*. 2011;35(12):2779–2787. https://doi.org/10.1007/s00268-011-1264-7
5. DeOliveira ML, Pawlik TM, Gleisner AL, Assumpcaom L, Lopes-Filho GJ, Choti MA. Echogenic appearance of colorectal liver metastases on intraoperative ultrasonography is associated with survival after hepatic resection. *J Gastrointest Surg*. 2007;11(8):970-976. https://doi.org/10.1007/s11605-007-0093-3
6. Auer RC, White RR, Kemeny NE, et al. Predictors of a true complete response among disappearing liver metastases from colorectal cancer after chemotherapy. *Cancer*. 2010;116(6):1502-1509. https://doi.org/10.1002/cncr.24912
7. Penney GP, Blackall JM, Hamady MS, Sabharwal T, Adam A, Hawkes DJ. Registration of freehand 3D ultrasound and magnetic resonance liver images. *Med Image Anal*. 2004;8(1):81-91.
8. Wein W, Brunke S, Khamene A, Callstrom MR, Navab N. Automatic CT-ultrasound registration for diagnostic imaging and image-guided intervention. *Med Image Anal*. 2008;12(5):577-585. https://doi.org/10.1016/j.media.2008.06.006
9. Banz VM, Müller PC, Tinguely P, et al. Intraoperative image-guided navigation system: development and applicability in 65 patients undergoing liver surgery. *Langenbeck's Arch Surg*. 2016;401(4):495-502. https://doi.org/10.1007/s00423-016-1417-0
10. Banz VM, Baechtold M, Weber S, Peterhans M, Inderbitzin D, Candinas D. Computer planned, image-guided combined resection and ablation for bilobar colorectal liver metastases. *World J Gastroenterol*. 2014;20(40):14992-14996. https://doi.org/10.3748/wjg.v20.i40.14992
11. Beller S, Lange T, Eulenstein S, et al. 3D-Elaboration of postoperative CT data after liver resection: technique and utility. *Int J Comput Assist Radiol Surg*. 2008;3(6):581-589. https://doi.org/10.1007/s11548-008-0262-1
12. Mozaffari MH, Lee W-S. Freehand 3-D ultrasound imaging: a systematic review. *Ultrasound Med Biol*. 2017;43(10):2099-2124. https://doi.org/10.1016/j.ultrasmedbio.2017.06.009
13. Nam WH, Kang DG, Lee D, Lee JY, Ra JB. Automatic registration between 3D intra-operative ultrasound and pre-operative CT images of the liver based on robust edge matching. *Phys Med Biol*. 2012;57(1):69–91. https://doi.org/10.1088/0031-9155/57/1/69
14. Lee D, Nam WH, Lee JY, Ra JB. Non-rigid registration between 3D ultrasound and CT images of the liver based on intensity and gradient information. *Phys Med Biol*. 2011;56(1):117–137. https://doi.org/10.1088/0031-9155/56/1/008
15. Neshat H, Cool DW, Barker K, Gardi L, Kakani N, Fenster A. A 3D ultrasound scanning system for image guided liver interventions. *Med Phys*. 2013;40(11):112903.
16. Lange T, Papenberg N, Heldmann S, et al. 3D ultrasound-CT registration of the liver using combined landmark-intensity information. *Int J Comput Assist Radiol Surg*. 2009;4(1):79–88. https://doi.org/10.1007/s11548-008-0270-1
17. Jago J, Chenal C, Jong J. XRES ®: adaptive enhancement of ultrasound images. *Medicamundi*. 2002;(November):36-41.
18. NVKF. Leidraad Kwaliteitscontrole Radiologische Apparatuur (Quality Control Guideline for Radiological Equipment). 2019. https://nvkf.nl/resources/LeidraadKwaliteitscontroleRadiologischeApparatuur3.0.pdf
19. Thijssen JM, Weijers G, de Korte CL. Objective performance testing and quality assurance of medical ultrasound equipment. *Ultrasound Med Biol*. 2007;33(3):460–471. https://doi.org/10.1016/j.ultrasmedbio.2006.09.006
20. Ivashchenko O, Smit J, Nijkamp J, et al. Clinical implementation of in-house developed MR-based patient-specific 3D models of liver anatomy. *Eur Surg Res*. 2021;61(4-5):143-152. https://doi.org/10.1159/000513335
21. Ivashchenko OV, Rijkhorst E-J, ter Beek LC, et al. A workflow for automated segmentation of the liver surface, hepatic vasculature and biliary tree anatomy from multiphase MR images. *Magn Reson Imaging*. 2020;68:53–65. https://doi.org/10.1016/j.mri.2019.12.008
22. Kikinis R, Pieper SD, Vosburgh KG. 3D slicer: a platform for subject-specific image analysis, visualization, and clinical support. In: *Intraoperative Imaging and Image-Guided Therapy*; 2014:277-289. https://doi.org/10.1007/978-1-4614-7657-3_19
23. Coulon P, de Brouwer F, Müller D, Steinberg A, Valette P. *Clinical Uses for CT Liver Analysis Application (White Paper)*. 2013. Accessed August 05, 2020. http://incenter.medical.philips.com/doclib/enc/fetch/2000/4504/577242/577251/587787/CT_Liver_Analysis.pdf%3fnodeid%3d10208979%26vernum%3d-2.
24. Lee TC, Kashyap RL, Chu CN. Building skeleton models via 3-D medial surface axis thinning algorithms. *CVGIP Graph Model Image Process*. 1994;56(6):462–478. https://doi.org/10.1006/cgip.1994.1042
25. Myronenko A, Song X. Point set registration: coherent point drifts. *IEEE Trans Pattern Anal Mach Intell*. 2010;32(12):2262-2275. https://doi.org/10.1109/TPAMI.2010.46
26. Lange T, Eulenstein S, Hünerbein M, Schlag PM. Vessel-based non-rigid registration of MR/CT and 3D ultrasound for navigation in liver surgery. *Comput Aided Surg*. 2003;8(5):228–240. https://doi.org/10.3109/10929080309146058
27. Thomson BR, Smit JN, Ivashchenko OV, et al. MR-to-US Registration Using Multiclass Segmentation of Hepatic Vasculature with a Reduced 3D U-Net. 2020. https://doi.org/10.1007/978-3-030-59716-0_27

How to cite this article: Smit JN, Kuhlmann KFD, Thomson BR, Kok NFM, Fusaglia M, Ruers TJM. Technical note: Validation of 3D ultrasound for image registration during oncological liver surgery. *Med. Phys.* 2021;00:1–8. https://doi.org/10.1002/mp.15080